7-1-2014

COLD INDUCIBLE RNA BINDING PROTEIN IS DISRUPTED IN ER+PR+HER2- TUMORS

Grace Okello

Grace Anyango Okello
Candidate

Cell Biology and Physiology
Department

This thesis is approved, and it is acceptable in quality and form for publication:

Approved by the Thesis Committee:

Rebecca Hartley, Chairperson

Linda Cook

Kristina Trujillo

COLD INDUCIBLE RNA BINDING PROTEIN IS DISRUPTED IN $ER^{+}PR^{+}HER2^{-}$ BREAST TUMORS

BY

GRACE A. OKELLO

B.S. MEDICAL LABORATORY SCIENCES

MBARARA UNIVERSITY OF SCIENCE AND TECHNOLOGY, 2008

THESIS

Submitted in Partial Fulfillment of the

Requirements for the Degree of

Master of Science

Biomedical Sciences

The University of New Mexico
Albuquerque, New Mexico

July, 2014

ACKNOWLEDGMENTS

I heartily acknowledge my mentor, Rebecca S. Hartley, PhD, for her patient instruction and continued encouragement throughout this project. Her friendly, caring and professional styles are things I admire and hope to emulate as I continue my career.
I wish to also thank my committee members Linda Cook, PhD, and Kristina Trujillo, PhD, for their valuable input into my research project.
To Huining Kang, PhD, thank you for your time and valuable instructions concerning the data analysis.
To Tamara Howard, MSc., thank you for the valuable instructions you gave in the technical aspects of laboratory procedures that were essential to this project.
To my friend and labmate Selina Garcia, thank you for contributing to this project in every way possible.
And finally to my beloved family and husband Kevin, thank you for being my number one fan.

COLD INDUCIBLE RNA BINDING PROTEIN IS DISRUPTED IN $ER^+PR^+HER2^-$ BREAST TUMORS

BY

GRACE A. OKELLO

B.S. MEDICAL LABORATORY SCIENCES, 2008

M.S. BIOMEDICAL SCIENCES, UNIVERSITY OF NEW MEXICO, 2014

ABSTRACT

RNA binding proteins (RBPs) and microRNAs (miRNAs) control gene expression post-transcriptionally by targeting mRNAs for translational activation, repression, or degradation. To date, aberrant expression of RBPs and miRNAs has been observed in many types of human cancers. We have shown the overexpression of Cold Inducible RNA binding protein (CIRP) in human breast cancer cell lines as compared to nontumorigenic and nontransformed breast epithelial cells. Others have shown cytoplasmic CIRP to be upregulated in a subset of breast tumors. Little is known about CIRP targets or its role in breast cancer. RBP Human antigen R (HuR), whose cytoplasmic localization is associated with aggressive breast cancer, and miR-125a, which is decreased in breast cancer, also have a poorly understood contribution to the etiology of breast cancer. Our studies in breast cancer cell lines have shown that CIRP overexpression upregulates HuR and proliferation, whereas miR-125a expression

downregulates HuR and suppresses proliferation. In this study, we address whether this post-transcriptional regulatory network is disrupted in clinical samples of human breast tumors by assessing the nuclear to cytoplasmic distribution of HuR, CIRP and miR-125a in three primary breast tumor subtypes: $ER^+PR^+HER2^-$, ER^+HER2^- and $ER^-PR^-HER2^-$, and matched normal breast tissue. Results show that the nuclear to cytoplasmic ratio of CIRP was increased in $ER^+PR^+HER2^-$ tumors compared to normal matched tissues, while HuR and miR-125a nuclear to cytoplasmic ratios show no significant difference between the tumors and matched normal tissues. The nuclear to cytoplasmic ratio of HuR is increased in the $ER^-PR^-HER2^-$ tumors compared to the other tumor subtypes, and this ratio correlates positively with proliferation. HuR and CIRP nuclear to cytoplasmic ratios positively correlate in $ER^+PR^+HER2^-$ tumors as do HuR and miR-125a nuclear to cytoplasmic ratios. Lastly, the nuclear to cytoplasmic ratio of miR-125a is decreased in ER^-HER2^+ tumors compared to $ER^+PR^+HER2^-$ tumor subtype. This brings us to the conclusion that the post transcriptional regulatory network is relevant to $ER^+PR^+HER2^-$ tumors and the $ER^-PR^-HER2^-$ tumors.

Table of Contents

LIST OF FIGURES

LIST OF TABLES

CHAPTER ONE

INTRODUCTION

RNA Binding Proteins and MicroRNAs

Breast cancer is a disease of abnormal gene expression[1]. Regulators such as RNA binding proteins (RBPs) and microRNAs (miRNAs) have been shown to contribute to this abnormal gene expression at the post-transcriptional level [2] yet their combined contribution to breast cancer etiology is understudied. RBPs contain one or more RNA binding domains such as the RNA recognition motif (RRM), zinc finger domain or the double stranded RNA binding motif [3]. By binding double or single stranded target RNA to form ribonucleoprotein (RNP) complexes, RBPs play diverse roles in transcription, pre-mRNA splicing and polyadenylation as well as in RNA modification, transport, localization, translation, and decay [4].

Similar to some RBPs, noncoding miRNAs bind to target sequences in mature mRNAs to decrease their stability and/or translation [5]. miRNAs are synthesized from longer primary miRNA transcripts, processed in the nucleus by ribonucleases and exported to the cytoplasm as pre-miRNAs. pre-miRNA is further processed to yield a 22-nucleotide miRNA duplex. Within this duplex, the strand with lower stability in the 5' end (guide end) is unwound and loaded into an RNP inhibitory complex called the RNA–induced silencing complex (RISC) [6].

miRNAs have been shown to play roles in development, differentiation and disease [7, 8]. To date, aberrant expression of RBPs and miRNAs has been observed in many types of human cancers [8, 9]. This paper focuses on two RBPs that are upregulated or relocalized in breast cancer and a miRNA that is downregulated in breast cancer as described below.

Human Antigen R

Human Antigen R (HuR) is an RBP that stabilizes mRNAs of genes that regulate cell proliferation, angiogenesis, apoptosis, rapid inflammatory response and the stress response [10, 11]. HuR is expressed ubiquitously and is a member of the ELAV (Embryonic Lethal Abnormal Vision) family of RBPs. In response to stress, HuR shuttles from the nucleus to the cytoplasm to stabilize and promote translation of its target mRNAs [11-13]. HuR upregulation and cytoplasmic localization has been associated with breast, gastric, lung, uterine cervical, bladder, and prostate carcinomas [11]. Despite studies associating HuR expression with tumorigenesis, a recent study showed an inverse relationship in a mouse xenograft model [15]. This same study also showed that HuR overexpression in MDA-MB 231 breast cancer cells increased cellular growth in vitro [14]. These reports suggest that the role of HuR may differ, depending on its expression in certain tissues or cell lines. Although primarily a nuclear protein, HuR stabilizes mRNAs in the cytoplasm, and elevated cytoplasmic HuR is associated with high histologic grade and poor survival of patients with breast, ovarian, colon and gastric adenocarcinomas [15-19]. Cytoplasmic HuR has also been implicated in tamoxifen resistance in breast cancer cells [20]. Despite its link to aggressive cancer and regulation

of cancer cell traits, little is known about the mechanisms that upregulate HuR in cancer.

Cold Inducible RBP

Cold-inducible RBP (CIRP), also known as heterogenous nuclear ribonucleoprotein A18 (A18 hnRNP), is also overexpressed in breast tumors and breast cancer cell lines [21, 22], as well as in other cancers [23]. CIRP binds the 5' or 3' untranslated region (UTR) of its target mRNAs to affect the rate of translational initiation and/or mRNA stability [23, 24]. CIRP is expressed in a wide variety of tissues and similarly to HuR, regulates proliferation, invasion, and migration, as well as inhibits apoptosis [25-27]. When induced by cellular stresses such as cold shock, UV irradiation and hypoxia, CIRP is upregulated and/or is shuttled from the nucleus into the cytoplasm to stabilize target mRNAs [22, 23, 27-32]. Our laboratory showed HuR to be a CIRP target. Overexpression of CIRP in breast cancer cells increased HuR levels, while knockdown of CIRP decreased HuR level [22]. Despite CIRP upregulation in breast tumors and cell lines, and its role in HuR regulation, CIRP's range of functions and other targets in normal mammary epithelia as well as in breast cancer are yet to be identified.

miR-125a

In contrast to overexpression of HuR and CIRP in breast cancer, miR-125a is reduced or mutated in cancers [33-36]. miR-125a has been shown to negatively regulate proliferation, invasion, and migration, and to promote apoptosis, and thus has been suggested as a tumor suppressor [8, 33-36]. Validated targets of miR-125a include ERBB2/ERBB3, HuR and p53 in human breast cancer cell lines; and MMP11, VEGF,

and Hepatitis B virus surface antigen in human liver cancers [33, 35, 37-40]. Our lab showed that miR-125a downregulated HuR in several different breast cancer cell lines, which also decreased proliferation [22, 33].

Rationale for the study

In this study, we set out to examine the nuclear to cytoplasmic ratios of CIRP, HuR and miR125a in primary human breast tumors and matched normal breast tissue. This work is based on our previous studies showing upregulation of HuR by CIRP and downregulation of HuR by miR-125a [22, 33], as well as other studies showing individual disruption of these post-transcriptional regulators in breast cancer, This study is the first step towards determining whether this post-transcriptional regulatory network as depicted in Figure 1, is disrupted in clinical samples of breast tumors and therefore potentially contributes to tumorigenesis. We hypothesize that the nuclear to cytoplasmic ratios of CIRP and HuR will be decreased in the tumors compared to their matched normal tissues, due to increased cytoplasmic protein, and that miR-125a will be decreased in the cytoplasm. We further hypothesize that these altered ratios will correlate positively with proliferation as well as with each other.

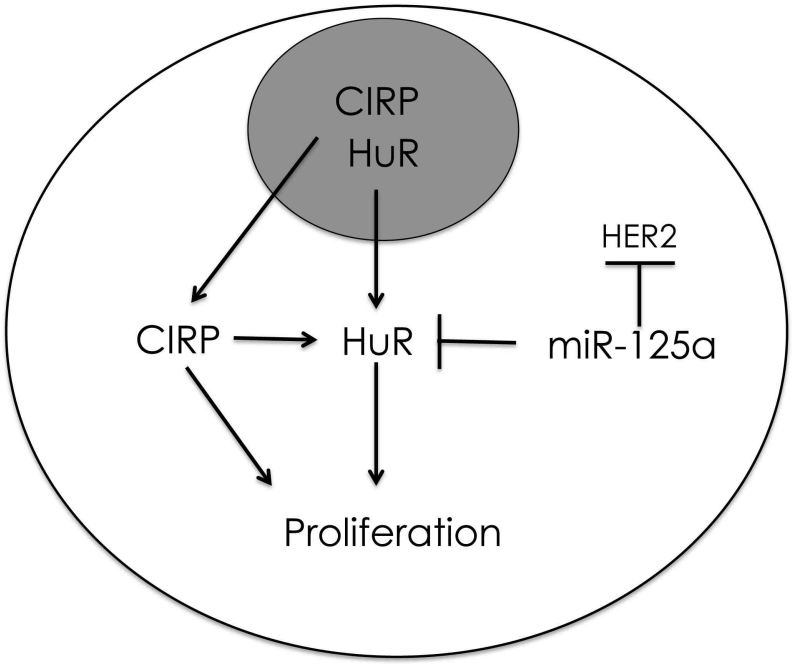

Figure 1: Schematic diagram showing the post-transcriptional regulatory network identified in breast cancer cell lines. The large circle represents a cell; the small gray circle represents the nucleus. CIRP and HuR have been shown to shuttle from the nucleus into the cytoplasm under cellular stress. CIRP upregulation in breast cancer cells increases HuR levels via an unknown mechanism and promotes cell proliferation, either directly or via increasing HuR [22]. Conversely, miR-125a negatively regulates HuR and suppresses cell proliferation [33]. miR-125a has also been shown to downregulate HER2 in breast cancer cell lines [38].

CHAPTER TWO
MATERIALS AND METHODS

Tissue Samples

The human breast tissue microarrays (TMAs) used for this study were constructed by the University of New Mexico Human Tissue Repository core facility (UNM HTR). Approval to pursue this study was granted by the University of New Mexico Human Research Review Committee (HRRC#10-058). The samples consisted of 75 primary breast tumors and matched, histologically normal adjacent breast tissue from patients who underwent treatment for breast cancer at the University of New Mexico Hospital and the University of New Mexico Cancer Research and Treatment Center. Two of the 75 patients received neoadjuvant treatment. Two pathologists examined and categorized the tumors according to their histological type as 70 invasive adenocarcinomas and 5 ductal carcinomas in-situ. Tumors were classified depending on the presence (+) or absence (-) of the estrogen receptor (ER), progesterone receptor (PR) and human epidermal growth factor receptor 2 (HER2). Subtypes included 25 of each $ER^+PR^+HER2^-$, ER^-HER2^+ and $ER^-PR^-HER2^-$ tumors and matched, histologically normal adjacent tissue. The pathologists also selected areas of each block to be cored. These cores were taken from archival formalin-fixed, paraffin-embedded blocks. Each TMA contained duplicate two mm diameter cores, two from the tumor and two from the matched normal tissue, for a total of four cores per patient. The total number of samples analyzed (*n*) was sometimes less than 25 as a result of sample loss during the staining process.

Immunofluorescence Analysis

Double immunofluorescence labeling (CIRP/HuR, CIRP/Ki67 and HuR/Ki67) was performed on sections from the TMAs. Commercially available primary antibodies were as follows: mouse monoclonal anti-HuR, clone 3A2 (10μg/ml, sc-5261, Santa Cruz Biotechnology, Santa Cruz, CA); rabbit monoclonal anti-Ki67, clone SP6 (10μg/ml, RM-9106-S0, Thermo Fisher Scientific, Fremont, CA); and mouse monoclonal anti-CIRBP (10μg/ml, 60025-1, Proteintech Group, Chicago, IL). Rabbit polyclonal actin antibody (H-300) (10μg/ml, sc-10731, Santa Cruz Biotechnology) was used as positive control. Negative controls included isotype-matched immunoglobulin as the primary antibody and omission of the primary antibody.

Five-micrometer-thick sections on slides were de-paraffinized in Hemo-De (product HD-150, batch 01313, Scientific Safety Solvents, Keller, TX) and immersed in 100% ethanol twice for 10 minutes each to remove the Hemo-De solution. To rehydrate, slides were passed sequentially tough a series 90% and 70% ethanol, and water (2 x 2 minutes). Antigen retrieval was performed in the microwave for 10 minutes using TET solution (10mM Tris pH 9.0, 1mM EDTA and 0.05% Tween-20) initially at full power, then lowered to prevent the solution from boiling. All slides were then washed in phosphate buffered saline (1X PBS) and blocked using 1X PBS, 3% normal goat serum (NGS) and 0.1% Triton X-100. Sections were incubated overnight with the primary antibody at 4°C in 1X PBS, 3% NGS, 0.1% Tween-20 and washed the next morning in PBS and 0.1% Tween-20 (PBST). Next, sections were incubated with the appropriate secondary antibody: goat anti-mouse-Alexa Fluor 488 (10µg/ml, catalog number A-11001,

Invitrogen/Life Technologies); goat anti-mouse Alexa Fluor 594 (10µg/ml, A-21044, Invitrogen/ Life Technologies), or goat anti-rabbit-Alexa Fluor 488 (10µg/ml, A-11034, Invitrogen/Life Technologies) for 1 hour in the dark then washed 2 x 10 minutes in PBST. Finally, sections were washed in a solution of 1X PBS containing the nuclear counterstain 4', 6-Diamidino-2-Phenylindole, Dihydrochloride (DAPI, 15ng/ml, catalog number D1306, Invitrogen/Life Technologies). Sections were mounted using ProLong Gold antifade reagent (P36930, Invitrogen/Life Technologies), cured for 3 hours at room temperature, sealed with nail polish and stored at 4°C.

Fluorescence In-Situ Hybridization

The microRNA fluorescence in situ hybridization (FISH) method was adapted from Planell-Saguer *et al*. 2010 [41]. A digoxigenin-labeled antisense LNA-oligodeoxynucleotide probe (40nM, product number 38521-15, miRCURY LNA, EXIQON Woburn, MA) for human miR-125a-5p with the sequence /5DigN/-TCACAGGTTAAAGGGTCTCAGGGA/3Dig_N/ was used for detection. An LNA-oligodeoxynucleotide scrambled probe with the sequence /5DigN/GTGTAACACGTCTATACGCCCA/3Dig_N/ double-DIG labeled was used as the negative control (40nM, product number 99004-15), while an anti-sense U6 snRNA LNA-oligodeoxynucleotide 5' DIG-labeled probe /5DigN/CACGAATTTGCGTGTCATCCTT/3Dig_N/ (1nM, product number 99002-15) was used as a positive control. Probe was omitted for an additional negative control.

Five-micrometer thick TMA sections mounted on positively charged slides were baked at 65°C for 2 hours and stored at 4°C for later use. Sections were de-paraffinized in Hemo-De, washed twice in 100% ethanol and rehydrated by passing the slides sequentially through 95% ethanol for 10 minutes, 70%, 50% and 30% ethanol for 5 minutes each and twice in water. Antigen retrieval was performed as described above. Sections were pre-hybridized in 3% NGS, 4X SSC and 10% dextran sulphate at 55°C for 20 minutes and hybridized in the same solution plus one of the above probes for 1hour. Washes were performed in the dark at 60°C with agitation as follows: 3 x 5 minutes with 4X SSC, 0.1% Tween-20; 1 x 5 minutes with 2X SSC; 1 x 5 minutes with 1X SSC. The final wash was at room temperature in PBS for 5 minutes. To block endogenous peroxidase activity, sections were treated for 20 minutes in 3% H_20_2 in PBS. Sections were then incubated in anti-DIG monoclonal rabbit antibody (10μg/ml, clone 9H27L19, 700772, Invitrogen/Life Technologies) solution (1X PBS, 3% NGS, 0.1% Tween-20) for 30 minutes at room temperature followed by a wash with TN buffer (0.1M Tris-HCl pH 7.5, 0.15M NaCl) in the dark with shaking for 5 minutes. Sections were then incubated for 30 minutes at room temperature in blocking solution (3% NGS, 0.1% Triton X-100 in PBS) followed by HRP-conjugated goat anti-rabbit IgG (25μg/ml, TSA kit #12, T20922, Invitrogen/Life Technologies) for 30 minutes at room temperature, and washed in TNT buffer (0.1M Tris-HCl pH 7.5, 0.15M NaCl, 0.2% Triton X-100) 3 times for 5 minutes each in the dark with shaking. Sections were then incubated at room temperature in Tyramide signal amplification solution for 10 minutes in darkness (TSA kit component as per manufacturer's instructions), washed 3 times in TNT buffer for 5 minutes followed by a

final 5 minutes wash in PBS containing DAPI (15ng/ml) and mounted with coverslips using ProLong Gold antifade reagent, treated and stored as described above.

Image analysis

Slides were viewed on a Zeiss Axioskop2 microscope equipped for epifluorescence using Chroma filter set 31000v2- AT350/50x (blue), 400dclp (green) and D460/50m (red) and photographed with a Coolsnap ES digital camera. Photographs of three random fields of each TMA core that contained epithelial ducts/tumor tissue were taken with a 40X objective. Exposure times for each antibody/probe (CIRP, HuR, miR-125a, actin and control antibodies) were optimized and all the images of that antibody were taken at the same exposure.

HuR, CIRP and miR-125a localization was evaluated using ImageJ (version 1.47d) imaging software from the NIH (http://imagej.nih.gov/ij/docs/guide/user-guide.pdf). Three 40X fields were used for analysis of each. DAPI nuclear staining was used to select images with epithelial ducts (normal samples) or tumor tissue (tumors) to avoid bias due to the antibody signal. For each field, DAPI images were manually thresholded and converted to a DAPI staining mask. The DAPI staining mask was inverted and then subtracted from the antibody stained image using the Image Calculator function in ImageJ to define the nuclear staining. A region of interest (ROI) containing epithelial ducts or tumor tissue was then selected from the CIRP or HuR stained image and also applied to the masked image. Quantitative fluorescent data representing total mean staining intensity (ROI of original image) and nuclear mean staining intensity (ROI of

subtracted image) were exported from ImageJ to Microsoft Excel. Cytoplasmic mean staining intensity was calculated by subtracting nuclear form total mean intensity.

In instances where image subtraction resulted in residual cytoplasmic staining, ROIs were selected for the nucleus and cytoplasm of between 10-20 individual cells. This method was also used to quantitate nuclear and cytoplasmic miR-125a. For this method, the stained image, DAPI image and a grid were overlain and colorized.

Circular ROIs were created to select the nucleus and the adjacent cytoplasm of individual cells. Cells that intersected corners of the grid were chosen to minimize selection bias. Quantitative fluorescent data representing nuclear and cytoplasmic mean staining intensities were exported from ImageJ to Microsoft Excel. For both methods, the nuclear to cytoplasmic ratio (N:C) was calculated for each field of each TMA core by dividing the nuclear mean staining intensity by the cytoplasmic mean staining intensity. Six fields were used in calculating ratios for each tumor or normal tissue, except in the case of missing cores or cores without epithelial or tumor tissues

Lastly, to determine the percentage of proliferating cells, Ki67 positive cells were counted, divided by the total number of DAPI stained nuclei and multiplied by 100.

.

Statistics

Data were graphed and statistically analyzed using GraphPad Prism (version 4.0a, GraphPad Software). $ER^+PR^+HER2^-$, ER^-HER2^+ and $ER^-PR^-HER2^-$ tumor subtypes and matched normal tissues were compared for nuclear to cytoplasmic ratio of HuR, CIRP, and miR-125a using a paired t test. Differences were considered statistically significant for p values ≤ 0.05. One-way analysis of variance (ANOVA) was used to compare CIRP, HuR or miR-125a levels between the 3 tumor subtypes followed by Tukey's multiple comparison analysis to determine specific differences in between tumors. Pearson's correlation coefficient r was used to determine relationships between Ki67/HuR, Ki67/CIRP, Ki67/miR-125a, HuR/CIRP, HuR/miR-125a and CIRP/miR-125a.

CHAPTER THREE

RESULTS

A previous study assessed CIRP expression in human breast, prostate and colon tumors [22]. CIRP was reported as present in 11 of 33 breast tumors (8/26 infiltrating carcinomas and 3/7 in situ carcinomas) and was mostly cytoplasmic. This study did not assess CIRP level in normal breast tissue, although it compared CIRP expression in prostate and colon tumors and matched normal tissues. In contrast, another study reported that CIRP was decreased in 12 endometrial hyperplasias and 39 carcinomas as compared to 27 normal endometria, where it was mostly nuclear and inversely correlated to proliferation [32]. We showed that CIRP was increased in 6 human breast cancer cell lines, as compared to nontumorigenic and nontransformed human mammary epithelial cells [22]. In the current study, we assessed the nuclear to cytoplasmic ratio of CIRP, HuR, or miR-125a using immunofluorescence analysis or FISH in breast tumors and normal matched tissue, as well as compared its nuclear to cytoplasmic ratio in different breast tumor subtypes that represent the least to the most aggressive tumors.

We chose to use immunofluorescence analysis/FISH as fluorescence can be quantitated to compare relative protein or RNA level. We chose to quantitate nuclear to cytoplasmic ratios as opposed to total levels due to the inherent difficulties of studying formalin-fixed, paraffin-embedded archival tissue. These difficulties include little control over how tissues were handled prior to fixation, fibrous or fibrotic tissues, and selection of cores by an independent pathologist. Although tissue microarrays are an excellent way to compare many different samples, the core is not always representative of the entire sample and

even duplicate cores can be quite variable. Selecting individual areas or cells to compare the relative level of the protein or miRNA in the nucleus and cytoplasm allowed for exclusion of areas of high background fluorescence due to fibrous tissue, capillaries or other irregularities in the microscopic fields within each core.

CIRP nuclear to cytoplasmic ratio is increased in $ER^+PR^+HER2^-$ tumors compared to normal matched tissue

Figure 2 shows representative micrographs of immunofluorescence staining of CIRP in breast tumors and adjacent normal tissues. CIRP was present in both the nucleus and cytoplasm of breast tumor cells and epithelial cells of adjacent normal tissues. CIRP levels and relative localization varied in both tumor and normal tissue, with some tumor and epithelial cells devoid of staining. Qualitatively, CIRP level appeared to be higher in tumors compared to normal breast tissues. Normal tissues adjacent to $ER^+PR^+HER2^-$ tumors appeared to have less CIRP staining in the epithelial cells compared to normal adjacent tissues to ER^-HER2^+ (Figure 2). In addition, tumors of all three subtypes appeared to have more cytoplasmic CIRP as compared to the normal tissues and nuclear CIRP also appeared more intense.

The ratio of CIRP in the nucleus vs. the cytoplasm (nuclear to cytoplasmic CIRP ratio, N:C) was significantly increased in $ER^+PR^+HER2^-$ tumors compared to matched normal tissues (Table 1 and Figure 3). Even though nuclear CIRP appeared more intense in tumors compared to normal matched tissues (Figure 2), there was no significant difference observed in the N:C CIRP ratio in ER^-HER2^+ and $ER^-PR^-HER2^-$ tumors

compared to matched normal tissues (Table 1). One-way analysis of variance (ANOVA) showed no significant difference in N:C CIRP ratio between the tumor subtypes.

CIRP ratios varied between fields within cores of the same patient (not shown), as well as between individual cells within the same field. Figure 4 shows an example of the CIRP nuclear to cytoplasmic ratio of 12 different cells within the same field of an $ER^{-}HER2^{+}$ tumor or normal tissue core. This example shows that this ratio is fairly constant in the normal tissue but varies greatly in the individual tumor cells.

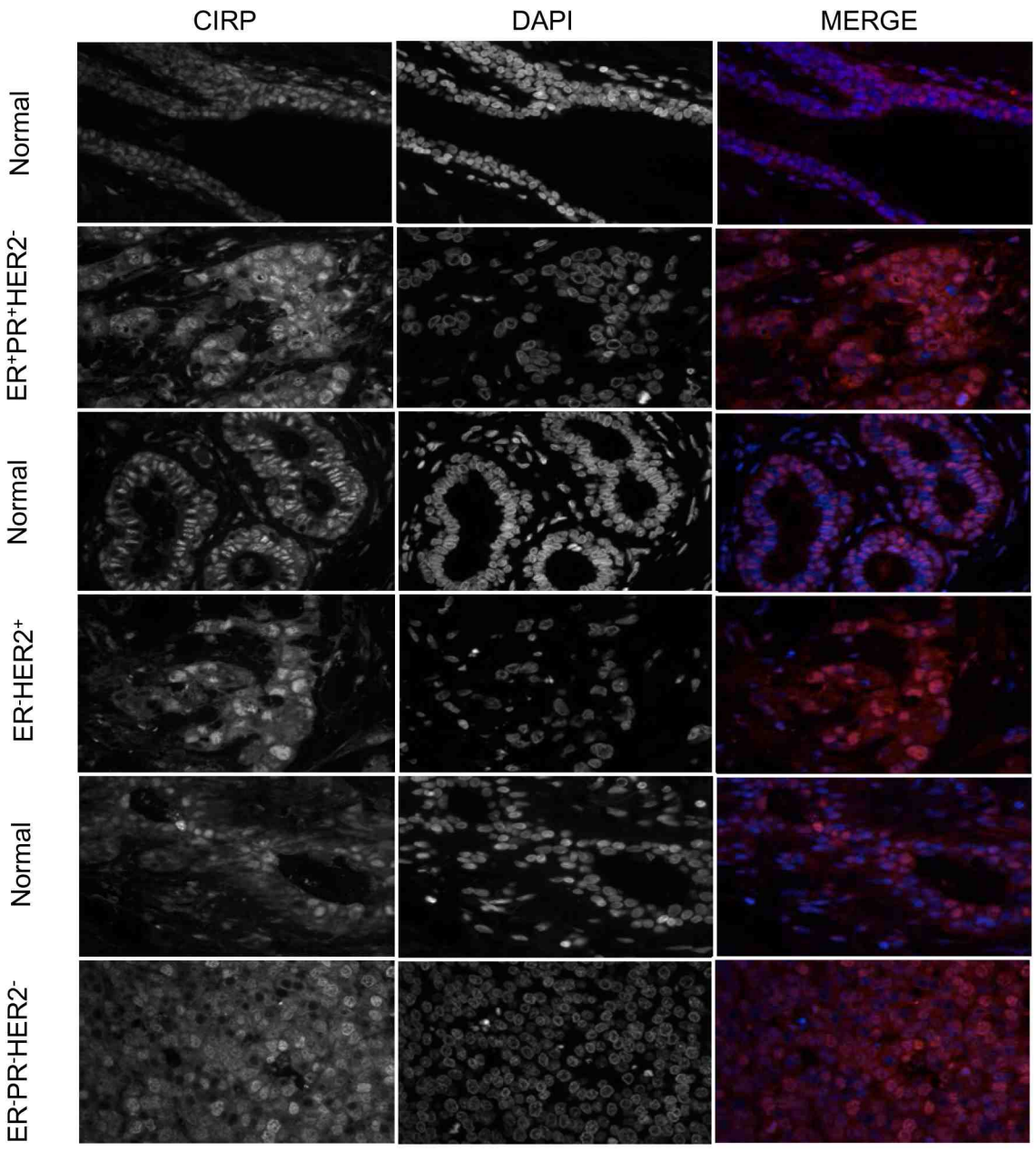

Figure 2: Representative images of CIRP immunofluorescence analysis in $ER^{+}PR^{+}HER2^{-}$, ER+HER2-, and ER-PR-HER2- breast tumors and matched normal tissue. Merge shows a colorized image of both CIRP and DAPI. Slides were viewed using a Zeiss Axioskop2 upright microscope and images were taken at 40X using a Coolsnap ES digital camera.

.

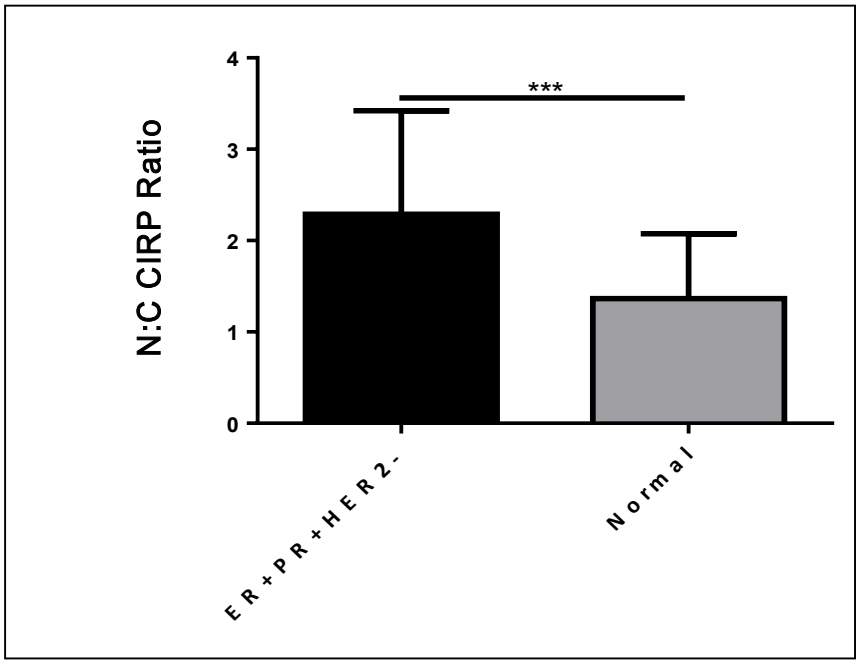

Figure 3: Bar graph of nuclear to cytoplasmic (N:C) CIRP ratio in $ER^{+}PR^{+}HER2^{-}$ tumors and normal matched tissues. *** p=0.0003 was determined using a paired t test.

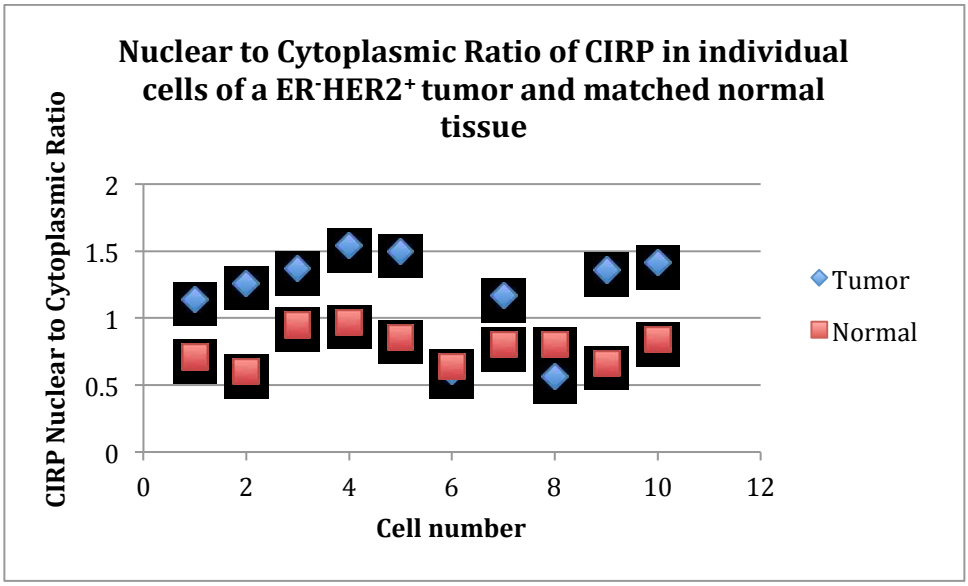

Figure 4. Graph of the nuclear to cytoplasmic ratio of CIRP in 12 separate cells from either a $ER^{-}HER2^{+}$ tumor or matched normal tissue. The x-axis represents 12 cells from either the tumor or normal tissue whose nuclear and cytoplasmic HuR was assessed. p= 0.003 (unpaired t test).

Table 1. Nuclear to cytoplasmic CIRP ratio in breast tumors and matched normal tissue

Tumor Subtype	nuclear to cytoplasmic ratio	Paired t-test	*n*
ER+PR+HER2-	2.29	0.0003***	19
Normal Adjacent	1.36		19
ER-HER2+	2.16	0.12	21
Normal Adjacent	1.96		21
ER-PR-HER2-	2.18	0.3	23
Normal Adjacent	1.91		23

* $p \leq 0.05$ is considered significant, n is less than 25 as some paired samples were lost during tissue processing.

Nuclear to cytoplasmic HuR ratio is similar in tumors and matched normal tissues.

Several studies have reported increased cytoplasmic HuR in a subset of breast cancers using immunohistochemistry [16, 42-45]. Only one of these studies assessed cytoplasmic and nuclear HuR levels in both tumors and normal breast tissue [45]. This study reported that, of the 82 breast tumors studied, 63 (76.8%) showed nuclear, 38 (46.3%) cytoplasmic and 28 (34.1%) showed both nuclear and cytoplasmic HuR expression. It also reported that, 18 of the 20 normal matched tissues they assessed showed strong nuclear staining, as did 14 of 16 fibro-adenomas. In addition, only 1 of the 20 normal matched tissues had cytoplasmic staining. This study assessed nuclear and cytoplasmic HuR expression by assigning scores dependent on the qualitative intensity of the staining. They did not determine the nuclear to cytoplasmic ratio of HuR in either tumor or normal tissue. In order to perform a more comprehensive analysis of HuR nuclear and cytoplasmic localization in both tumors and normal tissue, as well as to compare these values with those of CIRP, we next used immunofluorescence staining to assess the nuclear to cytoplasmic ratio of HuR in our breast tumor and matched normal breast tissue microarrays.

Immunofluorescence analysis showed that HuR, similar to CIRP was present in both the nucleus and cytoplasm of tumor cells and normal epithelial cells of adjacent normal tissues (Figure 5). The staining intensity varied with every patient and tumor subtype. $ER^+PR^+HER2^-$ tumors and matched normal tissues showed qualitatively less HuR staining compared to other subtypes, and this staining was primarily nuclear (Figure 4). In the normal tissue adjacent to ER^-HER2^+ tumors, the HuR levels of epithelial cells

within the same or adjacent duct varied. $ER^-PR^-HER2^-$ tumors appeared to have increased cytoplasmic staining compared to adjacent normal tissue and the other tumor subtypes.

Quantification of the nuclear to cytoplasmic HuR ratio showed no significant differences between the tumors and their normal matched tissues (Table 2). This observation may be due the averaging of the nuclear to cytoplasmic ratio of all patients within a tumor subtype. These ratios varied between fields within cores of the same patient (not shown), as well as between individual cells within the same field. Figure 6 shows an example of the HuR nuclear to cytoplasmic ratio of 10 different cells within the same field of an ER^-HER2^+ tumor or normal tissue core, This example shows that this ratio is fairly constant in the normal tissue but varies greatly in the individual tumor cells.

One-way ANOVA showed significant differences in the nuclear to cytoplasmic HuR ratio between the tumor subtypes ($p=0.03$) (Figure 6). This difference was confirmed using Tukey's multiple comparison test, which showed that the $ER^-PR^-HER2^-$ tumors had a higher nuclear to cytoplasmic ratio compared to $ER^+PR^+HER2^-$ tumors.

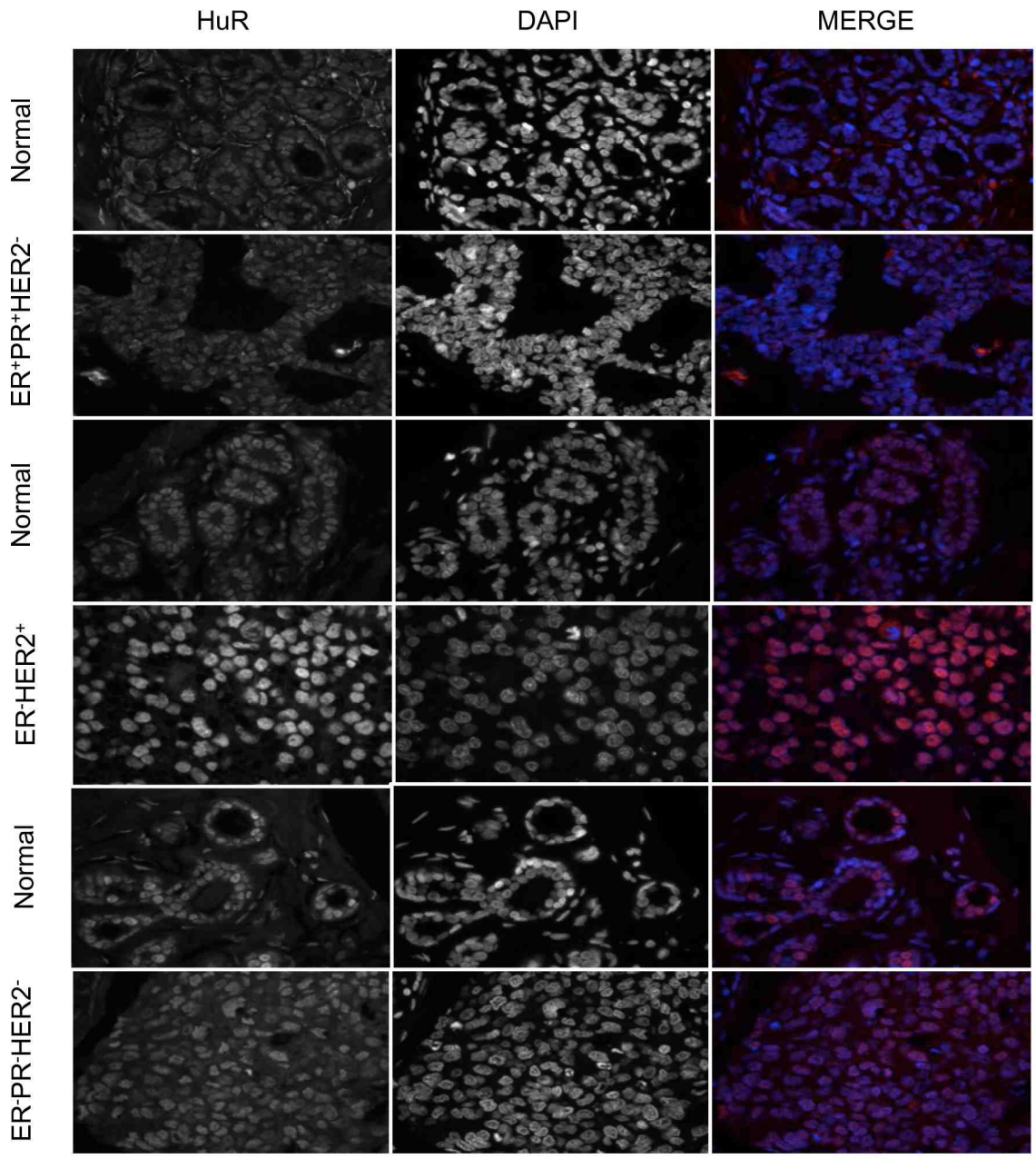

Figure 5: Representative images of HuR immunofluorescence analysis in $ER^+PR^+HER2^-$, ER^+HER2^-, and $ER^-PR^-HER2^-$ breast tumors and matched normal tissue. Merge shows a colorized image of both HuR and DAPI. Slides were viewed using a Zeiss Axioskop2 upright microscope and images were taken at 40X using a Coolsnap ES digital camera.

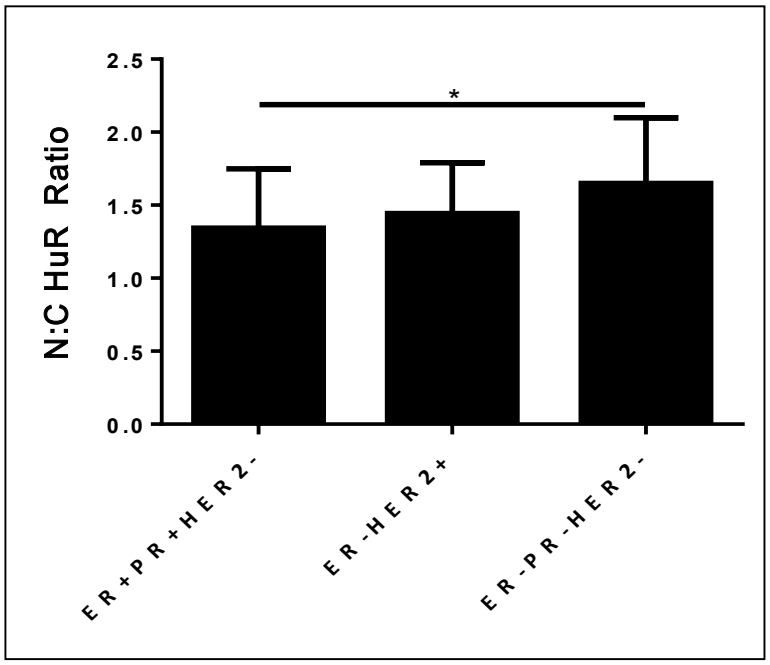

Figure 6: Bar graph of nuclear to cytoplasmic (N:C) HuR ratio in $ER^{+}PR^{+}HER2^{-}$, $ER^{-}HER2^{+}$, $ER^{-}PR^{-}HER2^{-}$ tumors. *p= 0.03 was determined with a one way ANOVA test.

Table 2. Nuclear to cytoplasmic HuR ratio in breast tumors vs. matched normal tissue

Tumor Subtype	nuclear to cytoplasmic ratio	Paired t-test	*n*
ER+PR+HER2-	1.34	0.49	21
Normal Adjacent	1.44		21
ER-HER2+	1.44	0.41	20
Normal Adjacent	1.47		20
ER-PR-HER2-	1.65	0.08	22
Normal Adjacent	1.48		22

Table 3. Multiple comparison test for HuR

Tumor Subtypes	p-value
$ER^+PR^+HER2^-$ vs. ER^-HER2^+	NS
$ER^+PR^+HER2^-$ vs. $ER^-PR^-HER2^-$	< 0.05*
ER^-HER2^+ vs. $ER^-PR^-HER2^-$	NS

* significant; NS means not significant

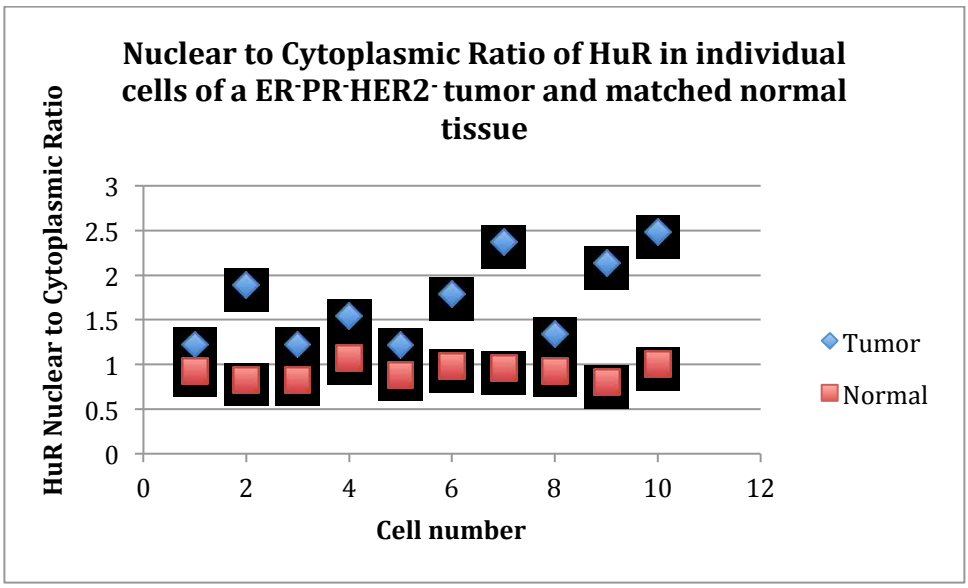

Figure 7. Graph of the nuclear to cytoplasmic ratio of HuR in 20 separate cells from either a ER^-HER2^+ tumor or matched normal tissue. The x-axis represents 20 cells from either the tumor or normal tissue whose nuclear and cytoplasmic HuR was assessed. p= 0.048 (unpaired t test).

Nuclear to cytoplasmic miR-125a ratio is constant

Lastly, we assessed miR-125a nuclear to cytoplasmic ratio using fluorescence in situ hybridization (FISH), in order to directly compare it to those of HuR and CIRP. miR-125a has been reported as reduced in both breast cancer cell lines and human breast tumors [8, 33, 36]. miR-125a has been shown to downregulate ERBB2 and ERBB3 in the SKBR3 breast cancer cell line to inhibit proliferation [37]. Our lab showed that miR-125a downregulated HuR in several different breast cancer cell lines, which also decreased proliferation [22, 33]. microRNAs have been shown to be localized in both the cytoplasm and the nucleus, where they perform different functions [48]. Given the cytoplasmic function of miR-125a in repressing translation of HuR, we predicted that the nuclear to cytoplasmic ratio of miR-125a would be increased due to decreased cytoplasmic miR-125a. This ratio may be lower in $HER2^+$ (ERBB2) expressing tumors in comparison to HER2 negative tumors since miR-125a also downregulates HER2.

FISH analysis showed miR-125a presence in both breast tumors and adjacent normal tissues (Figure 8). ER^-HER2^+ tumors and matched normal tissues showed reduced expression as compared to the $ER^+PR^+HER2^-$ and $ER^-PR^-HER2^-$ tumors. $ER^-PR^-HER2^-$ tumors showed more miR-125a expression compared to matched normal tissues. In general, the expression of miR-125a varied across patients as well as tumor subtypes.

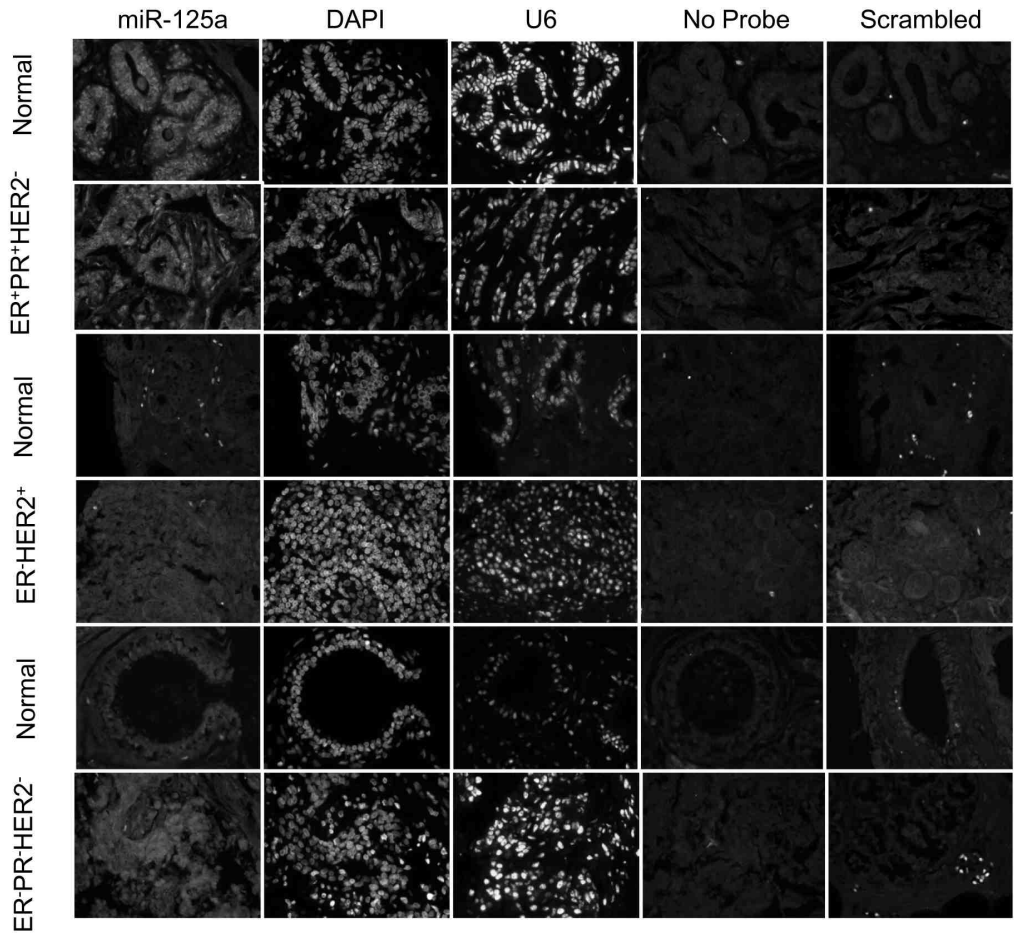

Figure 8: Representative images of miR-125a by FISH in $ER^{+}PR^{+}HER2^{-}$, ER+HER2-, and ER-PR-HER2- breast tumors and matched normal tissue. Slides were viewed using a Zeiss Axioskop2 upright microscope and images were taken at 40X using a Coolsnap ES digital camera.

Despite these qualitative differences in expression, there were no significant differences in the nuclear to cytoplasmic ratio of miR-125a between the $ER^+PR^+HER2^-$, ER^-HER2^+, $ER^-PR^-HER2^-$ tumors and matched normal tissue (Table 4), indicating that the localization of miR-125a is not different between tumors and normal tissue. In contrast, one-way ANOVA showed significant differences for miR-125a ($p=0.04$) across the 3 tumor subtypes (Figure 9). These differences were confirmed by multiple comparison tests (Table 5), which showed that $ER^+PR^+HER2^-$ tumors have a significantly higher nuclear to cytoplasmic ratio of miR-125a compared to ER^-HER2^+ tumors.

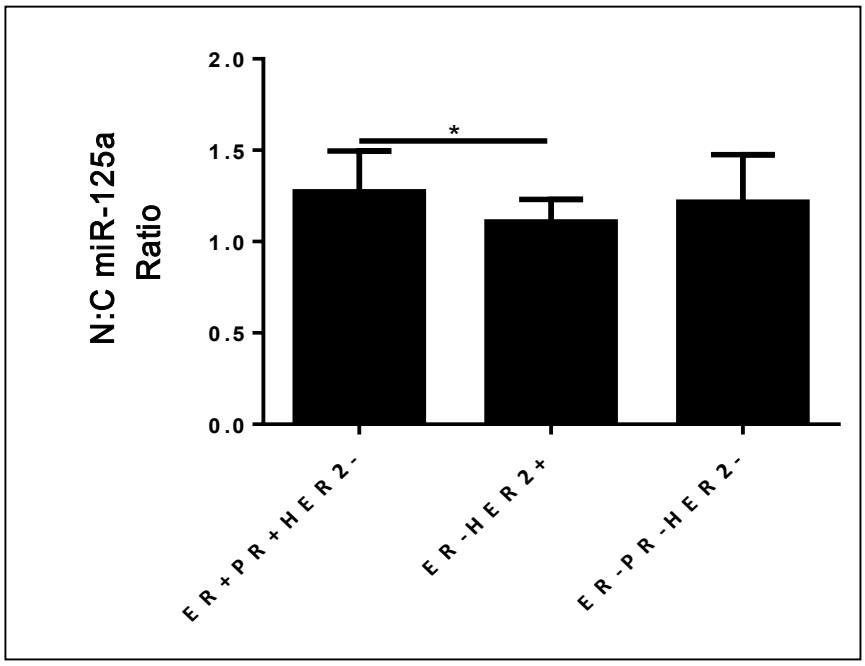

Figure 9: Bar graph of nuclear to cytoplasmic miR-125a ratio of breast tumors. *p= 0.04 was determined using a one way ANOVA test.

Table 4. Nuclear to cytoplasmic ratio of miR-125a in breast tumors vs. matched normal tissue.

Tumor Subtype	nuclear to cytoplasmic ratio	Paired t-test	*n*
$ER^+PR^+HER2^-$	1.27	0.73	22
Normal Adjacent	1.23		22
ER^-HER2^+	1.11	0.07	20
Normal Adjacent	1.04		20
$ER^-PR^-HER2^-$	1.22	0.80	21
Normal Adjacent	1.25		21

Table 5. Multiple comparison test for miR-125a

Tumor Subtypes	p-value
$ER^+PR^+HER2^-$ vs. ER^-HER2^+	< 0.05*
$ER^+PR^+HER2^-$ vs. $ER^-PR^-HER2^-$	NS
ER^-HER2^+ vs. $ER^-PR^-HER2^-$	NS

* significant; NS means not significant

HuR weakly correlates with proliferation in $ER^-PR^-HER2^-$ tumors

Both CIRP and HuR have been shown to stimulate proliferation in vitro, miR-125a to inhibit proliferation, and HuR to correlate positively with proliferation in tumors [22, 33]. To determine the relationship between CIRP, HuR and miR-125a as well as between each of these markers and proliferation (i.e., Ki67), we performed correlation analyses. Table 6 shows the results of correlation analysis in tumors, using nuclear to cytoplasmic ratio. HuR nuclear to cytoplasmic ratio correlated weakly with proliferation only in the $ER^-PR^-HER2^-$ tumors (r=0.475).

There was no correlation between the nuclear to cytoplasmic ratio of CIRP and Ki67, or of miR-125a and Ki67 in any of the tumors. CIRP nuclear to cytoplasmic ratio correlated weakly with that of HuR in the $ER^+PR^+HER2^-$ tumors (r=0.400). There was no correlation between the nuclear to cytoplasmic ratios of CIRP and miR-125a in any tumor subtype. HuR and miR-125a nuclear to cytoplasmic ratios showed a weak positive correlation in $ER^+PR^+HER2^-$ tumors (r=0.480).

Table 6. Correlation analysis in tumors using nuclear to cytoplasmic ratios

Tumor Subtype	Ki67/CIRP r value	Ki67/HuR r value	Ki67/miR-125a r value	CIRP/HuR r value	CIRP/miR-125a r value	HuR-miR-125a r value
$ER^{+}PR^{+}HER2^{-}$	0.265	-0.125	-0.237	0.400*	0.265	0.480*
$ER^{-}HER2^{+}$	0.041	-0.082	-0.089	-0.212	-0.119	-0.004
$ER^{-}PR^{-}HER2^{-}$	0.323	0.475*	-0.375	0.246	0.255	-0.124

* weak relationship

CHAPTER FOUR

DISCUSSION

The independent expression of CIRP, HuR and miR125a has been studied in breast tumors and breast cancer cell lines. Overall, these studies showed that both HuR and CIRP protein levels, and cytoplasmic localization, are increased in a subset of breast tumors, while miR-125a expression is decreased. The expression or localization of these post-transcriptional regulators has not been assessed within the same breast tumors. In addition, studies have shown that cytoplasmic HuR correlates with high tumor grade [15, 16] as well as ER^-PR^- [44] and $ER^+PR^+HER2^+$ [45] status in human breast cancers. Our laboratory previously showed HuR protein and proliferation to be upregulated by CIRP [33] and downregulated by miR-125a in breast cancer cell lines [22]. Based on these collective reports, we hypothesized that cytoplasmic CIRP and cytoplasmic HuR would be increased, and miR-125a decreased in a subset of tumors and in comparison to matched normal tissues. We also hypothesized that increased cytoplasmic CIRP and HuR (a lower nuclear to cytoplasmic ratio) would correlate positively with proliferation while increased cytoplasmic miR-125a would correlate negatively with proliferation.

In this study, we show that CIRP is localized both in the nucleus and cytoplasm of normal breast epithelial cells and human breast tumor cells where its presence and level varies. Our results do not support our hypothesis, as CIRP nuclear to cytoplasmic ratio is increased in $ER^+PR^+HER2^-$ breast tumors compared to normal adjacent tissues. This increase could be due to an increase of nuclear CIRP with no change in cytoplasmic, a decrease in cytoplasmic with no change in nuclear CIRP, or an increase in nuclear and

decrease in cytoplasmic CIRP. CIRP is known to shuttle from the nucleus into the cytoplasm in response to stress, such as hypoxia and DNA damage [23]. In the cytoplasm it binds and stabilizes target mRNAs and/or increases their translation. Tumor cells often survive in a hypoxic environment with underlying DNA damage, thus our prediction of increased cytoplasmic CIRP in tumors compared to normal tissues. One possibility is that the nuclear to cytoplasmic CIRP is higher because of a nuclear CIRP function, as CIRP has been shown to bind DNA as well as RNA [23].

Our findings show that although CIRP level and localization varies, it is predominantly nuclear in both tumors and normal matched tissue. Qualitatively, tumors appear to have increased cytoplasmic CIRP compared to matched normal tissue. Although the nuclear to cytoplasmic ratios of ER^-HER2^+ and $ER^-PR^-HER2^-$ tumors were not significantly different than normal adjacent tissues, an increase in both cytoplasmic and nuclear CIRP could explain this result. In support of this, nuclear CIRP also appears higher in tumors. A careful analysis within each patient comparing the nuclear to cytoplasmic ratio of cells between all fields assessed could help determine if CIRP nuclear to cytoplasmic ratio is significantly different between normal tissue and tumor of a specific patient. Regardless, this is the first study to assess nuclear to cytoplasmic CIRP ratio in normal breast tissue.

The nuclear to cytoplasmic ratios of HuR indicate that it is predominantly nuclear in both tumors and normal matched tissues. Our results also show that tumor and some normal tissues had cytoplasmic staining. Several studies have shown increased cytoplasmic HuR in aggressive breast cancers, but only one assessed nuclear and cytoplasmic HuR in both

tumors and normal breast tissue [45]. In that study, 63 of 82 breast tumors (76.8%) showed nuclear HuR, 38 (46.3%) cytoplasmic and 28 (34.1%) showed both nuclear and cytoplasmic HuR [45]. Of 20 normal matched tissues, 18 (90%) showed strong nuclear staining, and only 1(5%) had cytoplasmic staining. [45]. Our results differ because we are studying nuclear to cytoplasmic ratios and not just the presence or absence of HuR in the cytoplasm [45].

Our results also showed that there was no significant difference in the nuclear to cytoplasmic HuR ratio between tumors and normal matched tissue. This was surprising, as qualitatively, the $ER^-PR^-HER2^-$ tumors had increased HuR in the cytoplasm while the ER^-HER^+ tumors had the highest nuclear staining.

It is possible that tissue adjacent to tumor, although histologically normal, may not be normal by other criteria. It is becoming clear that histologically normal breast tissue may be genetically abnormal [1] and that these perturbations may play significant roles in the early stages of breast cancer. A recent study reported upregulation of inducers of an epithelial to mesenchymal transition in tumor-adjacent, histologically normal breast tissues located 1 centimeter from the margins of breast adenocarcinomas, as compared to 5 centimeter away [46]. Our normal adjacent tissues were collected at least 1cm from the breast tumor margin. Thus, the observed similarities in the nuclear to cytoplasmic ratio of HuR between tumors and matched normal tissues could be because these normal tissues are not genetically normal.

Several studies have reported that miR-125a is deregulated in breast tumors and breast

cancer cell lines [8, 33, 35, 36, 47]. These studies assessed miR-125a expression using microarray analysis [36], qRT-PCR [33, 35, 36], or northern analysis [33, 35, 36]. One of these studies reported a decrease of miR-125a in breast tumors versus normal breast tissues [36]. Our laboratory previously reported miR125a was decreased and HuR increased in breast cancer cell lines [34]. In the current study, FISH analysis shows that miR-125a expression appears lower in $ER^{-}HER2^{+}$ and $ER^{-}PR^{-}HER2^{-}$ tumors compared to $ER^{+}PR^{+}HER2^{-}$ tumors. The nuclear to cytoplasmic ratios in tumors as compared to normal matched tissues were not significantly different, suggesting that it is not regulated at the level of localization.

When we compared nuclear to cytoplasmic miR-125a ratio between the tumor subtypes, we found that $ER^{-}HER2^{+}$ tumors had a significantly decreased nuclear to cytoplasmic ratio of miR-125a compared to $ER^{+}PR^{+}HER2^{-}$ tumors. This result agrees with published reports of miR-125a downregulating HER2 in breast cancer cell lines.

A recent study reported that mature miRNAs can shuttle to the nucleus from the cytoplasm where they directly target primary miRNA transcripts and small nuclear RNAs to regulate their biogenesis and function [48]. Another study reported miR-125a as more concentrated in the nucleolus compared to the nucleoplasm and cytoplasm [49]. We did not determine the subnuclear localization of miR-125a, but its presence in the nucleus in both normal and tumor tissue is supported by these previous studies.

We had hypothesized that CIRP and HuR would correlate positively with proliferation and with each other, while miR-125a would correlate negatively with proliferation. Our study shows that nuclear to cytoplasmic ratio of HuR and proliferation correlate positively in $ER^-PR^-HER2^-$ tumors while CIRP shows no correlation with proliferation in any of the tumors. These results indicate that CIRP nuclear to cytoplasmic ratio could not be used as a predictor of proliferation. ER-PR-HER2- tumors have the highest percentage of Ki67 positive cells (not shown) and the highest nuclear to cytoplasmic ratio of HuR, suggesting a causal relationship. This correlation is consistent with HuR's known function in promoting proliferation.

We also show that the nuclear to cytoplasmic ratio of CIRP and HuR correlate positively in the $ER^+PR^+HER2^-$ tumors, agreeing with our initial hypothesis. Interestingly, HuR and miR-125a nuclear to cytoplasmic ratios correlated positively in $ER^+PR^+HER2^-$ tumors. In our previous study of miR-125a regulation of HuR in breast cancer cell lines, we noted that one breast cancer cell line had high levels of both HuR and miR-125a. miR-125a localization was not assessed but HuR was nuclear [33]. miR-125a has several validated and many potential targets other than HuR [40]. There is also a known polymorphism (rs12976445) within the pri-miR-125a sequence correlating with the amount of mature hsa-miR-125a in breast tumors. Those with the rs12976445 variant (T/T) have higher levels of hsa-miR-125a in comparison to those with variants (C/T and C/C), who also have increased HER2 expression in breast tumors [35]. Future studies could determine if these variants are differentially localized in different breast tumor subtypes.

In summary, the nuclear to cytoplasmic expression patterns of HuR, CIRP and miR-125a were examined along with proliferative index in tissue microarrays of three primary breast tumor subtypes- ($ER^+PR^+HER2^+$, ER^-HER2^+ and $ER^-PR^-HER2^-$)- and their matched normal breast tissues. Our results showed that nuclear to cytoplasmic CIRP ratio was increased in $ER^+PR^+HER2^-$ tumors compared to normal tissue. HuR and CIRP nuclear to cytoplasmic ratios were positively correlated in the same tumor subtype as were those of HuR and miR-125a. HuR nuclear to cytoplasmic ratio also positively correlated with proliferation in $ER^-PR^-HER2^-$ tumors. When tumors subtypes were compared, miR-125a was seen as decreased in ER^-HER2^+ tumors. Future studies will assess intra-tumor variability in order to further understand how disruption of this post-transcriptional network can be used to potentially predict outcome or treatment of $ER^+PR^+HER2^-$ tumors, especially as the majority of these tumors in our study were already invasive.

This was a pilot study that involved 25 paired samples of 3 different tumor subtypes and normal matched tissues. As a result, larger studies are warranted to further understand this post-transcriptional network. This study was done with limited clinical and pathological data: the tumor histopathology (invasive lobular, ductal or ductal carcinoma in situ) and receptor status. We will obtain information on age, race, menopausal status, tumor size, histological grade, tumor stage, survival and treatment, pending availability for future analyses. We will also assess the intra-tumor variability to understand if the post-transcriptional network can be used to predict outcome/treatment of patients with $ER^+PR^+HER2^-$ tumors or other tumor subtypes.

REFERENCES

1. Tripathi A, King C, de la Morenas A, Perry VK, Burke B, Antoine GA, Hirsch EF, Kavanah M, Mendez J, Stone M *et al*: **Gene expression abnormalities in histologically normal breast epithelium of breast cancer patients**. *Int J Cancer* 2008, **122**(7):1557-1566.

2. Ciafre SA, Galardi S: **microRNAs and RNA-binding proteins: a complex network of interactions and reciprocal regulations in cancer**. *RNA Biol* 2013, **10**(6):935-942.

3. Lunde BM, Moore C, Varani G: **RNA-binding proteins: modular design for efficient function**. *Nature reviews Molecular cell biology* 2007, **8**(6):479-490.

4. Glisovic T, Bachorik JL, Yong J, Dreyfuss G: **RNA-binding proteins and post-transcriptional gene regulation**. *FEBS Lett* 2008, **582**(14):1977-1986.

5. Ambros V: **The functions of animal microRNAs**. *Nature* 2004, **431**(7006):350-355.

6. Ma JB, Yuan YR, Meister G, Pei Y, Tuschl T, Patel DJ: **Structural basis for 5'-end-specific recognition of guide RNA by the A. fulgidus Piwi protein**. *Nature* 2005, **434**(7033):666-670.

7. Ruan K, Fang X, Ouyang G: **MicroRNAs: novel regulators in the hallmarks of human cancer**. *Cancer letters* 2009, **285**(2):116-126.

8. O'Day E, Lal A: **MicroRNAs and their target gene networks in breast cancer**. *Breast cancer research : BCR* 2010, **12**(2):201.

9. Kim MY, Hur J, Jeong S: **Emerging roles of RNA and RNA-binding protein network in cancer cells**. *BMB Rep* 2009, **42**(3):125-130.

10. Abdelmohsen K, Gorospe M: **Posttranscriptional regulation of cancer traits by HuR**. *Wiley interdisciplinary reviews RNA* 2010, **1**(2):214-229.

11. Wang J, Guo Y, Chu H, Guan Y, Bi J, Wang B: **Multiple Functions of the RNA-Binding Protein HuR in Cancer Progression, Treatment Responses and Prognosis**. *Int J Mol Sci* 2013, **14**(5):10015-10041.

12. Gallouzi IE, Brennan CM, Stenberg MG, Swanson MS, Eversole A, Maizels N, Steitz JA: **HuR binding to cytoplasmic mRNA is perturbed by heat shock**. *Proceedings of the National Academy of Sciences of the United States of America* 2000, **97**(7):3073-3078.

13. Wang W, Furneaux H, Cheng H, Caldwell MC, Hutter D, Liu Y, Holbrook N, Gorospe M: **HuR regulates p21 mRNA stabilization by UV light**. *Molecular and cellular biology* 2000, **20**(3):760-769.

14. Gubin MM, Calaluce R, Davis JW, Magee JD, Strouse CS, Shaw DP, Ma L, Brown A, Hoffman T, Rold TL *et al*: **Overexpression of the RNA binding protein HuR impairs tumor growth in triple negative breast cancer associated with deficient angiogenesis**. *Cell cycle* 2010, **9**(16):3337-3346.

15. Denkert C, Weichert W, Pest S, Koch I, Licht D, Kobel M, Reles A, Sehouli J, Dietel M, Hauptmann S: **Overexpression of the embryonic-lethal abnormal vision-like protein HuR in ovarian carcinoma is a prognostic factor and is associated with increased cyclooxygenase 2 expression**. *Cancer Res* 2004, **64**(1):189-195.

16. Heinonen M, Bono P, Narko K, Chang SH, Lundin J, Joensuu H, Furneaux H, Hla T, Haglund C, Ristimaki A: **Cytoplasmic HuR expression is a prognostic factor in invasive ductal breast carcinoma**. *Cancer Res* 2005, **65**(6):2157-2161.

17. Erkinheimo TL, Lassus H, Sivula A, Sengupta S, Furneaux H, Hla T, Haglund C, Butzow R, Ristimaki A: **Cytoplasmic HuR expression correlates with poor outcome and with cyclooxygenase 2 expression in serous ovarian carcinoma**. *Cancer Res* 2003, **63**(22):7591-7594.

18. Yoo PS, Sullivan CA, Kiang S, Gao W, Uchio EM, Chung GG, Cha CH: **Tissue microarray analysis of 560 patients with colorectal adenocarcinoma: high expression of HuR predicts poor survival**. *Annals of surgical oncology* 2009, **16**(1):200-207.

19. Mrena J, Wiksten JP, Thiel A, Kokkola A, Pohjola L, Lundin J, Nordling S, Ristimaki A, Haglund C: **Cyclooxygenase-2 is an independent prognostic factor in gastric cancer and its expression is regulated by the messenger RNA stability factor HuR**. *Clin Cancer Res* 2005, **11**(20):7362-7368.

20. Hostetter C, Licata LA, Witkiewicz A, Costantino CL, Yeo CJ, Brody JR, Keen JC: **Cytoplasmic accumulation of the RNA binding protein HuR is central to tamoxifen resistance in estrogen receptor positive breast cancer cells**. *Cancer biology & therapy* 2008, **7**(9):1496-1506.

21. Artero-Castro A, Callejas FB, Castellvi J, Kondoh H, Carnero A, Fernandez-Marcos PJ, Serrano M, Ramon y Cajal S, Lleonart ME: **Cold-inducible RNA-binding protein bypasses replicative senescence in primary cells through extracellular signal-regulated kinase 1 and 2 activation**. *Molecular and cellular biology* 2009, **29**(7):1855-1868.

22. Guo X, Wu Y, Hartley RS: **Cold-inducible RNA-binding protein contributes to human antigen R and cyclin E1 deregulation in breast cancer**. *Molecular carcinogenesis* 2010, **49**(2):130-140.

23. Lleonart ME: **A new generation of proto-oncogenes: cold-inducible RNA binding proteins**. *Biochim Biophys Acta* 2010, **1805**(1):43-52.

24. Al-Fageeh MB, Smales CM: **Cold-inducible RNA binding protein (CIRP) expression is modulated by alternative mRNAs**. *Rna* 2009, **15**(6):1164-1176.

25. Sakurai T, Itoh K, Higashitsuji H, Nonoguchi K, Liu Y, Watanabe H, Nakano T, Fukumoto M, Chiba T, Fujita J: **Cirp protects against tumor necrosis factor-alpha-induced apoptosis via activation of extracellular signal-regulated kinase**. *Biochim Biophys Acta* 2006, **1763**(3):290-295.

26. Saito K, Fukuda N, Matsumoto T, Iribe Y, Tsunemi A, Kazama T, Yoshida-Noro C, Hayashi N: **Moderate low temperature preserves the stemness of neural stem cells and suppresses apoptosis of the cells via activation of the cold-inducible RNA binding protein**. *Brain Res* 2010, **1358**:20-29.

27. Nishiyama H, Itoh K, Kaneko Y, Kishishita M, Yoshida O, Fujita J: **A glycine-rich RNA-binding protein mediating cold-inducible suppression of mammalian cell growth**. *The Journal of cell biology* 1997, **137**(4):899-908.

28. Sheikh MS, Carrier F, Papathanasiou MA, Hollander MC, Zhan Q, Yu K, Fornace AJ, Jr.: **Identification of several human homologs of hamster DNA damage-inducible transcripts. Cloning and characterization of a novel UV-inducible cDNA that codes for a putative RNA-binding protein**. *J Biol Chem* 1997, **272**(42):26720-26726.

29. Wellmann S, Buhrer C, Moderegger E, Zelmer A, Kirschner R, Koehne P, Fujita J, Seeger K: **Oxygen-regulated expression of the RNA-binding proteins RBM3 and CIRP by a HIF-1-independent mechanism**. *Journal of cell science* 2004, **117**(Pt 9):1785-1794.

30. De Leeuw F, Zhang T, Wauquier C, Huez G, Kruys V, Gueydan C: **The cold-inducible RNA-binding protein migrates from the nucleus to cytoplasmic stress granules by a methylation-dependent mechanism and acts as a translational repressor**. *Experimental cell research* 2007, **313**(20):4130-4144.

31. Yang C, Carrier F: **The UV-inducible RNA-binding protein A18 (A18 hnRNP) plays a protective role in the genotoxic stress response**. *J Biol Chem* 2001, **276**(50):47277-47284.

32. Hamid AA, Mandai M, Fujita J, Nanbu K, Kariya M, Kusakari T, Fukuhara K, Fujii S: **Expression of cold-inducible RNA-binding protein in the normal endometrium, endometrial hyperplasia, and endometrial carcinoma**.

International journal of gynecological pathology : official journal of the International Society of Gynecological Pathologists 2003, **22**(3):240-247.

33. Guo X, Wu Y, Hartley RS: **MicroRNA-125a represses cell growth by targeting HuR in breast cancer**. *RNA Biol* 2009, **6**(5):575-583.

34. Duan R, Pak C, Jin P: **Single nucleotide polymorphism associated with mature miR-125a alters the processing of pri-miRNA**. *Human molecular genetics* 2007, **16**(9):1124-1131.

35. Lehmann TP, Korski K, Ibbs M, Zawierucha P, Grodecka-Gazdecka S, Jagodzinski PP: **rs12976445 variant in the pri-miR-125a correlates with a lower level of hsa-miR-125a and ERBB2 overexpression in breast cancer patients**. *Oncology letters* 2013, **5**(2):569-573.

36. Iorio MV, Ferracin M, Liu CG, Veronese A, Spizzo R, Sabbioni S, Magri E, Pedriali M, Fabbri M, Campiglio M *et al*: **MicroRNA gene expression deregulation in human breast cancer**. *Cancer Res* 2005, **65**(16):7065-7070.

37. Scott GK, Goga A, Bhaumik D, Berger CE, Sullivan CS, Benz CC: **Coordinate suppression of ERBB2 and ERBB3 by enforced expression of micro-RNA miR-125a or miR-125b**. *J Biol Chem* 2007, **282**(2):1479-1486.

38. Zhang Y, Gao JS, Tang X, Tucker LD, Quesenberry P, Rigoutsos I, Ramratnam B: **MicroRNA 125a and its regulation of the p53 tumor suppressor gene**. *FEBS Lett* 2009, **583**(22):3725-3730.

39. Bi Q, Tang S, Xia L, Du R, Fan R, Gao L, Jin J, Liang S, Chen Z, Xu G *et al*: **Ectopic expression of MiR-125a inhibits the proliferation and metastasis of hepatocellular carcinoma by targeting MMP11 and VEGF**. *PLoS One* 2012, **7**(6):e40169.

40. Potenza N, Papa U, Mosca N, Zerbini F, Nobile V, Russo A: **Human microRNA hsa-miR-125a-5p interferes with expression of hepatitis B virus surface antigen**. *Nucleic Acids Res* 2011, **39**(12):5157-5163.

41. de Planell-Saguer M, Rodicio MC, Mourelatos Z: **Rapid in situ codetection of noncoding RNAs and proteins in cells and formalin-fixed paraffin-embedded tissue sections without protease treatment**. *Nature protocols* 2010, **5**(6):1061-1073.

42. Denkert C, Weichert W, Winzer KJ, Muller BM, Noske A, Niesporek S, Kristiansen G, Guski H, Dietel M, Hauptmann S: **Expression of the ELAV-like protein HuR is associated with higher tumor grade and increased cyclooxygenase-2 expression in human breast carcinoma**. *Clin Cancer Res* 2004, **10**(16):5580-5586.

43. Heinonen M, Fagerholm R, Aaltonen K, Kilpivaara O, Aittomaki K, Blomqvist C, Heikkila P, Haglund C, Nevanlinna H, Ristimaki A: **Prognostic role of HuR in hereditary breast cancer**. *Clin Cancer Res* 2007, **13**(23):6959-6963.

44. Heinonen M, Hemmes A, Salmenkivi K, Abdelmohsen K, Vilen ST, Laakso M, Leidenius M, Salo T, Hautaniemi S, Gorospe M *et al*: **Role of RNA binding protein HuR in ductal carcinoma in situ of the breast**. *The Journal of pathology* 2011, **224**(4):529-539.

45. Zhu Z, Wang B, Bi J, Zhang C, Guo Y, Chu H, Liang X, Zhong C, Wang J: **Cytoplasmic HuR expression correlates with P-gp, HER-2 positivity, and poor outcome in breast cancer**. *Tumour Biol* 2013, **34**(4):2299-2308.

46. Trujillo KA, Heaphy CM, Mai M, Vargas KM, Jones AC, Vo P, Butler KS, Joste NE, Bisoffi M, Griffith JK: **Markers of fibrosis and epithelial to mesenchymal transition demonstrate field cancerization in histologically normal tissue adjacent to breast tumors**. *Int J Cancer* 2011, **129**(6):1310-1321.

47. Potenza N, Russo A: **Biogenesis, evolution and functional targets of microRNA-125a**. *Molecular genetics and genomics : MGG* 2013, **288**(9):381-389.

48. Liang H, Zhang J, Zen K, Zhang CY, Chen X: **Nuclear microRNAs and their unconventional role in regulating non-coding RNAs**. *Protein Cell* 2013, **4**(5):325-330.

49. Politz JC, Hogan EM, Pederson T: **MicroRNAs with a nucleolar location**. *Rna* 2009, **15**(9):1705-1715.